INTERNATIONAL JOURNAL OF NOVEL RESEARCH AND DEVELOPMENT (IJNRD)
© 2026 IJNRD | Volume 11, Issue 4, April 2026 | ISSN: 2456-4184 | IJNRD.ORG

ROLE OF WATER–CEMENT RATIO AND ADMIXTURES IN IMPROVING MECHANICAL AND DURABILITY CHARACTERISTICS OF 3D PRINTED CONCRETE

Undapalli. Satya Durga[1], Guttula. Swathi[1], Sirra. Naveen Kumar[1], Bandaru. Veerendra[1], Korakuti Hanumanthu[2]

[1]UG Student, Civil Engineering Department, Bonam Venkata Chalamayya Engineering College, Odalarevu, Andhra Pradesh, India.

[2]Associate Professor, Civil Engineering Department, Bonam Venkata Chalamayya Engineering College, Odalarevu, Andhra Pradesh, India.

Abstract : 3D concrete printing (3DCP) is an emerging construction technology that enables automated layer-by-layer fabrication without the need for conventional formwork, reducing construction time, material waste, and labor requirements. This study investigates the influence of water–cement (w/c) ratio and various chemical and mineral admixtures on the mechanical strength and durability of 3D printable concrete. A Taguchi L9 orthogonal array was adopted to evaluate nine mix combinations with varying w/c ratios (0.30, 0.40, 0.50), superplasticizer dosages, silica fume content, and polypropylene fiber percentages, while maintaining fly ash at 20%. The mixes were tested for 28 - day compressive strength, sorptivity, saturation index, and surface porosity using ImageJ analysis. Results indicate that the mix with w/c ratio 0.40 and higher superplasticizer dosage achieved optimal performance, with maximum compressive strength of 29.5 N/mm² and improved durability characteristics. The study concludes that a balanced combination of w/c ratio and admixtures is essential for achieving desirable printability, strength, and durability in 3D concrete printing applications.

Key words - 3D printable concrete, Compressive Strength, Sorptivity, Saturation, ImageJ porosity analysis, Taguchi L9 array, Durability.

INTRODUCTION

The construction industry is experiencing a fundamental shift with the emergence of additive manufacturing technologies, and 3D concrete printing (3DCP) stands at the forefront of this change. By depositing concrete layer-by layer in an automated manner, 3DCP eliminates the need for traditional formwork — a development that translates directly into faster build times, reduced labor requirements, lower material wastage, and significantly greater freedom in architectural design [1][2]. Projects ranging from pedestrian bridges to multi-storey residential units have already been completed using this technology across multiple countries, signaling a broader commercial readiness [3].

Despite this progress, one of the most persistent engineering challenges in 3DCP is the development of a suitable concrete mix. The material must flow freely enough to be pumped and extruded through a nozzle without clogging, yet it must simultaneously develop sufficient rigidity to maintain the geometry of each deposited layer and bear the weight of subsequent layers - all without the support of any external formwork [4]. These two requirements are fundamentally in tension, and achieving the right balance requires careful control of the w/c ratio and the admixture system.

A higher w/c ratio improves flowability and eases extrusion but weakens the hardened structure and compromises layer stability. Conversely, a lower w/c ratio enhances compressive strength and durability but can render the mix too stiff to extrude reliably [5]. Chemical admixtures such as PCE-based superplasticizers and mineral additions including silica fume, fly ash, and polypropylene fibers offer practical levers to navigate this conflict - improving workability without sacrificing strength, and refining the internal pore structure to enhance long-term durability [6][7][8][9].

Although considerable research has examined these materials individually, there remains a lack of comprehensive, systematically designed studies that assess the combined influence of the w/c ratio and multiple additive types on the both mechanical performance and durability in the same experimental program [10]. Furthermore, advanced characterization tools such as ImageJ-based image porosity analysis and sorptivity testing - which provide direct insight into the microstructural and transport properties of hardened concrete - have not been widely applied in the 3DCP context [11][12]. This study addresses these gaps by adopting a Taguchi L9 experimental design to investigate nine concrete mixes with varying proportions, evaluating each through compressive strength testing, sorptivity,

saturation immersion, and surface pore analysis, with the aim of identifying optimum mix design parameters for practical 3D concrete printing.

LITERATURE REVIEW

The development of 3D printable concrete has gained widespread attention across the globe, with researchers focusing on improving its strength, workability, and durability. Early work by Le et al. [1] played a key role in advancing high-performance 3D concrete printing. They demonstrated that compressive strengths exceeding 100 MPa could be achieved using a carefully designed mix containing cement and polycarboxylate superplasticizer. Their optimized composition - 70% cement, 20% fly ash, and 10% silica fume - set an important benchmark for future studies.

Building on this, Kazemian et al. [2] focused on the fresh-state properties of 3D printable concrete, such as printability, shape stability, and surface quality. By incorporating a polycarboxylate-based high-range water reducer and a viscosity-modifying admixture in small quantities, they established practical guidelines for achieving stable and consistent extrusion. Similarly, Zhang et al. [3] highlighted the importance of aggregate optimization, showing a clear relationship between cement paste flowability and the ideal sand content required for maintaining buildability.

Further studies have explored the combined effects of admixtures. Manikandan et al. [4] demonstrated that polycarboxylate-based superplasticizers, when used alongside silica fume, can effectively improve yield stress while maintaining adequate viscosity, making the mix suitable for longer printing durations. Giridhar et al. [5] emphasized the practicality of 3DCP by proposing simple and cost-effective testing methods, making the technology more accessible, especially in developing regions.

Durability has also been a key area of focus. Rahul et al. [13] introduced the concept of “desorptivity” while studying water movement in cement mortar, highlighting the importance of sorptivity tests in understanding moisture behavior. Roussel [14] provided a theoretical framework for printable concrete by defining essential rheological parameters such as yield stress, viscosity, and structural build-up. Girskas and Kligys [15] further reinforced the importance of chemical admixtures, noting that components like superplasticizers and viscosity modifiers are essential for successful 3D printing.

In terms of microstructural analysis, Putten et al. [16] examined interlayer pore distribution in 3D printed materials, while Zhang et al. [17] used ImageJ software to establish a link between porosity and compressive strength. The sorptivity test, standardized under ASTM C1585 [18], is widely accepted as a reliable method to assess water absorption and durability. Chen et al. [19] showed that incorporating fly ash and silica fume can significantly reduce water absorption in 3DCP mixes.

More recent studies have also considered sustainability and optimization. Wang et al. [20] highlighted that using supplementary cementitious materials can reduce carbon emissions by up to 30 - 40% while improving durability. Mohan et al. [21] explored alternative binders, finding that calcium sulfoaluminate-based systems offer better buildability compared to conventional OPC mixes. Finally, Papachristoforou et al. [22] demonstrated the effectiveness of the Taguchi design approach in optimizing mix proportions, allowing researchers to obtain meaningful results with fewer experimental trials.

MATERIALS AND THEIR PROPERTIES

3.1 Cement

Ordinary Portland Cement (OPC) of 53 grade, conforming to IS 12269:1987, was used as the primary binder in all mixes. Standard preliminary tests confirmed a normal consistency of 30%, an initial setting time of 1 hour 5 minutes, a final setting time of 5 hours 23 minutes, a fineness of 3.87% - well within the permissible limit of 10% - and a specific gravity of 3.16. These properties confirm the suitability of the cement for use in 3D printable concrete applications.

3.2 Fine Aggregate

Sand passing through a 2 mm sieve, classified as Zone II per IS 383, was used as the fine aggregate. Testing per IS 2386 revealed a specific gravity of 2.46, fineness modulus of 2.87, and water absorption of approximately 1%. The Zone II classification indicates a balanced particle size distribution that supports good workability and print quality.

3.3 Chemical Admixtures

A polycarboxylate ether (PCE)-based superplasticizer with a specific gravity of 1.05 - 1.10 was incorporated at dosages of 0.2%, 1.0%, and 1.9% by weight of cement. Its primary function is to improve flowability and reduce water demand without compromising viscosity.

3.4 Mineral Additives

Silica fume with a specific gravity of 2.2 was added at 0.2%, 5.1%, and 10% by weight of the binder to improve compressive strength, reduce permeability, and refine the pore structure through its pozzolanic action. Fly ash with a specific gravity of 2.1–2.3 was incorporated at a constant replacement level of 20%, contributing to enhanced workability, reduced heat of hydration, and improved long-term durability.

3.5 Polypropylene Fibers

Polypropylene (PP) fibers were added at dosages of 0.1%, 0.65%, and 1.2% by weight of the binder. These fibers are known to control plastic shrinkage cracking, improve the green strength of freshly extruded layers, and enhance the ductility of the hardened concrete — all of which are beneficial in a 3D printing context.

EXPERIMENTAL METHODOLOGY

4.1 Experimental Design — Taguchi L9 Orthogonal Array

A Taguchi L9 orthogonal array was adopted to systematically evaluate five key factors - w/c ratio, superplasticizer (SP) dosage, silica fume (SF) content, polypropylene fiber content, and fly ash content - each at three levels, while minimizing the total number of experimental trials. Fly ash was held constant at 20% for all trials. Table I presents the factor levels used in the experimental design.

Table 1: Taguchi L9 array — factor levels for all nine trial mixes

Trial	W/C Ratio	SP%	SF%	Fiber(%)	Fly Ash(%)
1	0.30	0.2	0.2	0.10	20
2	0.30	1.0	5.1	0.65	20
3	0.30	1.9	10.0	1.20	20
4	0.40	0.2	5.1	1.20	20
5	0.40	1.0	10.0	0.10	20
6	0.40	1.9	0.65	0.65	20
7	0.50	0.2	0.65	0.65	20
8	0.50	1.0	1.20	1.20	20
9	0.50	1.9	0.10	0.10	20

4.2 Mix Proportions

All nine mixes maintained a constant cement-to-sand ratio of 1:2. For each trial, cube specimens (70×70×70 mm) and cylindrical specimens (100×50 mm) were cast. Materials were precisely weighed and dry-mixed manually in a mixing tray until uniform. Water, combined with the required superplasticizer dosage, was then added gradually while mixing continued until the batch achieved a smooth, cohesive consistency suitable for extrusion. The fresh concrete was then placed into oiled moulds in layers, with each layer compacted using a tamping rod to remove entrapped air.

Fig. 1: Mixing of 3D printable concrete

Fig. 2: Preparation of cylinders

Fig. 3: Preparation of cubes

Fig. 4: Compaction of 3DPC cubes

Fig. 5: Compaction of 3DPC cylinders

Fig. 6: Allowing specimens for setting

4.3 Curing

After casting, specimens were kept undisturbed for 24 hours before demoulding. They were then transferred to a water curing tank and submerged for 28-days. All specimens were removed from the curing tank immediately before testing to ensure consistent moisture conditions at the time of testing.

4.4 Compressive Strength Test

The 28 - day compressive strength of cube specimens was measured in accordance with IS 4031 (Part 6)-1988 using a compression testing machine. The maximum load at failure was recorded, and compressive strength was calculated by dividing this load by the cube cross-sectional area of 4900 mm² (70 mm cubes).

Fig. 7: Compressive strength test on trial 1 specimens

Fig. 8: Cube specimens before testing

Fig. 9: Cracking pattern observed

4.5 ImageJ-Based Surface Porosity Analysis

Surface pore analysis was carried out using ImageJ - an open-source image processing software developed by the National Institutes of Health, USA, widely used in concrete research. Surface photographs of each specimen were captured under consistent lighting at a fixed distance. The images were imported into ImageJ, converted to 8-bit grayscale, and a binary threshold (Otsu's method) was applied to distinguish pores (dark regions) from the solid matrix (light regions). Particle analysis was then performed to determine pore count, total pore area, average pore size, and percentage porosity.

Fig. 10: Surface images of specimens for ImageJ analysis

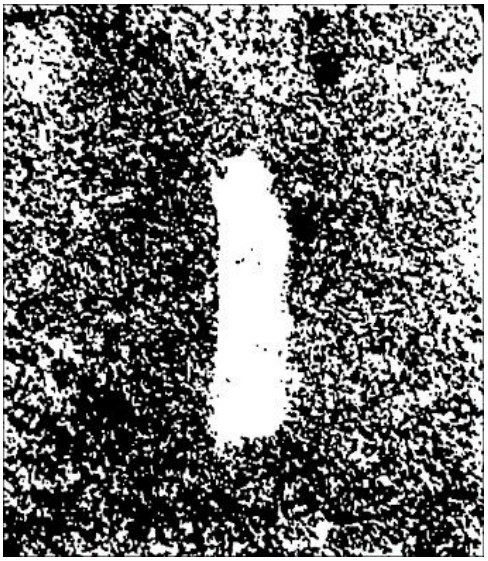

Fig. 11: Grayscale and thresholded image in ImageJ

4.6 Sorptivity Test (Water Absorption)

Sorptivity testing was carried out on cylindrical specimens (100×50 mm) to evaluate capillary water absorption as per ASTM C1585 and IS 9299 standards. Specimens were oven-dried at 105°C for 24 hours and conditioned before testing. The curved surfaces were sealed with aluminum foil tape to ensure unidirectional water flow. the bottom surface of each specimen was placed in shallow contact with water (depth 2 - 5 mm), and weights were recorded at regular intervals from 1 minute up to 8 days. The sorptivity coefficient was calculated from the linear relationship between cumulative absorption per unit area and the square root of elapsed time.

Fig. 12 : Oven drying of specimens

Fig. 13 : Sealing with aluminum tape

Fig. 14: Sorptivity test in progress — specimens placed in water tray

4.7 Saturation Test (Water Absorption by Immersion)

The saturation test was conducted as per IS 2386 Part III to assess the total water absorption capacity of each mix under full immersion. Cylindrical specimens of 100 mm diameter and 50 mm thickness were oven-dried at 40°C to a constant oven-dry weight (W_OD). They were then fully submerged in water and weighed daily for a continuous period of 8 days.

Fig. 15: Full immersion of cylindrical specimens for saturation test

RESULTS AND DISCUSSION

5.1 Compressive Strength

Table 2 presents the 28 - day compressive strength results for all nine trial mixes. Trial 6 (w/c = 0.40, SP = 1.9%, SF = 0.2%, fiber = 0.65%, fly ash = 20%) achieved the highest compressive strength of 29.5 N/mm², making it the best-performing mix across the entire test program. The higher superplasticizer dosage in this mix allowed the water demand to be reduced while maintaining flowability, resulting in a denser hardened matrix and superior strength. Trials 2, 4, and 5 each achieved 24.4 N/mm², while Trial 3 (w/c = 0.30 with 10% silica fume) recorded only 16.3 N/mm² - reflecting the over-stiffening effect of excessive silica fume at a very low w/c ratio. The w/c = 0.50 mixes (Trials 7–9) achieved strengths of 15.6–20.4 N/mm², confirming that excess water dilutes the cementitious matrix and increases porosity, reducing both strength and stability.

Table 2: 28-day compressive strength results for all nine trial mixes

Trial	W/C	CS Area (mm^2)	Load (kN)	Strength (N/mm^2)
1	0.30	4900	110	22.4
2	0.30	4900	120	24.4
3	0.30	4900	80	16.3
4	0.40	4900	120	24.4
5	0.40	4900	120	24.4
6	0.40	4900	145	29.5
7	0.50	4900	75	15.6
8	0.50	4900	100	20.4
9	0.50	4900	100	20.4

5.2 ImageJ Surface Porosity Analysis

Table 3 summarizes the image analysis results for all nine trial specimens. Trial 1 exhibited the lowest porosity percentage of 32.02% with an average pore size of 493.1 px^2, indicating a compact and well-distributed pore network despite its relatively modest compressive strength - a result that can be attributed to the very low w/c ratio of 0.30 producing minimal capillary voids. Trial 7 recorded the highest porosity (51.64%), consistent with its high w/c ratio of 0.50 and low silica fume content. The ImageJ results confirm that pore size distribution, rather than total porosity alone, governs concrete mechanical performance [11][23] - Trial 1 with 373 smaller pores outperformed Trial 4 with 394 larger pores (averaging 1442 px^2), even though both had similar pore counts.

Table 3: ImageJ surface porosity analysis results — all nine trial mixes

Trial	Pore Count	Total Area (px^2)	Avg. Size (px^2)	% Area (Porosity)
1	373	183,929	493.1	32.02
2	759	531,807	700.7	47.99
3	168	262,319	1561.4	41.82
4	394	568,228	1442.2	51.39
5	514	298,638	581.0	37.17
6	586	341,873	583.4	46.98
7	588	446,590	759.5	51.64
8	423	310,341	733.7	50.50
9	938	279,537	298.0	36.35

5.3 Sorptivity Results

The sorptivity test tracked weight gain in specimens over time as water was drawn in by capillary suction. Table I4 presents the sorptivity coefficients (Si) and R^2 values for each mix. Mixes with a lower w/c ratio of 0.30 showed slower initial water uptake and reached a stable weight much earlier, indicating a denser and less permeable pore network. The w/c = 0.50 mixes (Trials 7–9) continued absorbing water beyond 24 hours, pointing to a more open and connected pore structure. Trial 6 (w/c = 0.40) showed a balanced and moderate absorption rate with a sorptivity coefficient of 0.023, which was lower than the higher w/c mixes, confirming its superior durability performance. These findings are consistent with Chen et al. [19] and Neville [24], who reported that lower w/c ratios consistently reduce capillary water penetration.

Table 4: Sorptivity coefficients (S_i) and R^2 values for all nine trial mixes

Trial	Sorptivity (S_i) ($mm/sec^{0.5}$)	R^2
T1	0.100	0.963
T2	0.048	0.948
T3	0.011	0.912
T4	0.016	0.971
T5	0.017	0.988
T6	0.023	0.978
T7	0.030	0.991
T8	0.026	0.965
T9	0.022	0.991

The following figures (Fig. 20–28) show the cumulative water absorption versus the square root of time for all nine trial mixes, illustrating the rate of sorptivity and the point at which each mix reached effective moisture equilibrium.

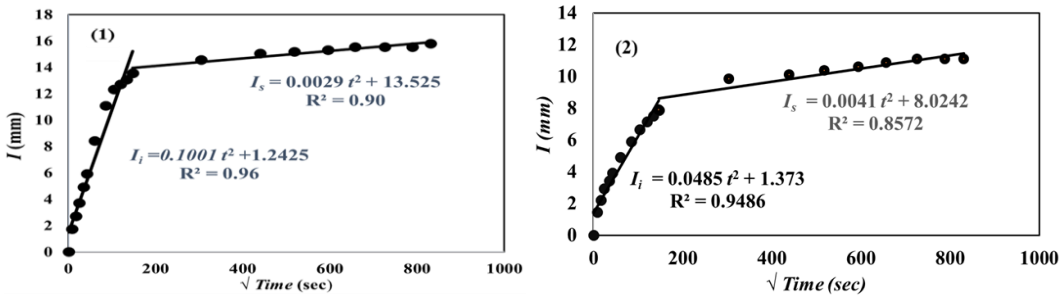

Fig. 16 and 17: Cumulative absorption vs √time — trials 1 and 2

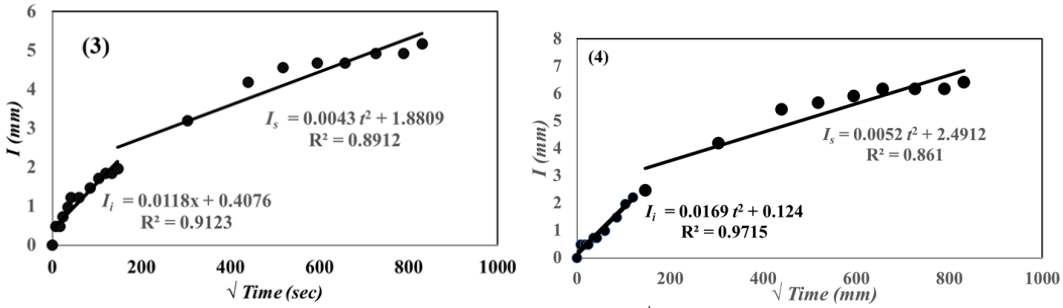

Fig. 18 and 19: Cumulative absorption vs √time — trials 3 and 4

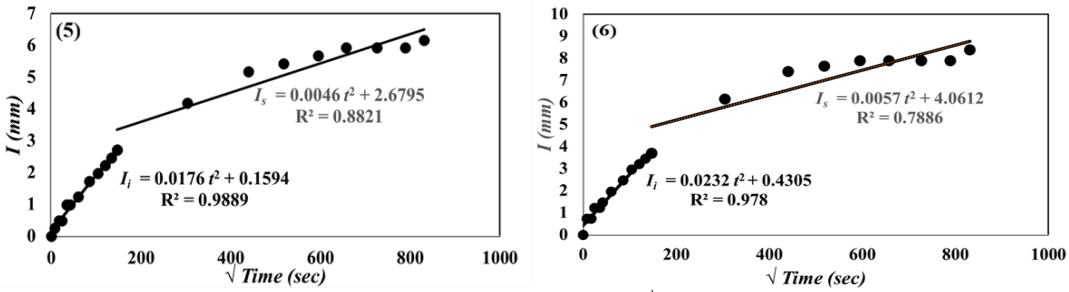

Fig. 20 and 21: Cumulative absorption vs √time — trials 5 and 6

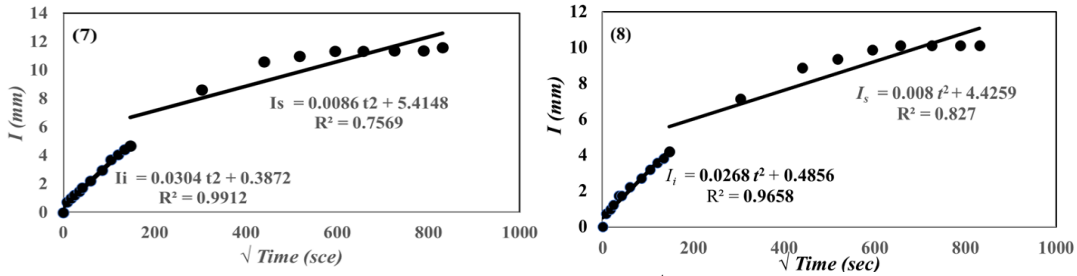

Fig. 22 and 23: Cumulative absorption vs √time — trials 7 and 8

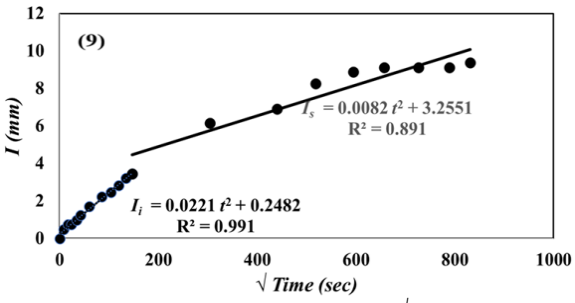

Fig. 24: Cumulative absorption vs √time — trial 9

5.4 Saturation Test Results

The saturation test was carried out on all nine trial mixes by fully immersing the specimens in water for eight consecutive days, from 01-03-2026 to 14-03-2026, as per IS 2386 Part III. The saturation index was obtained by dividing the total water absorbed by the specimen volume of 405.3655 cm³, providing a consistent basis for comparing all nine mixes.

Table 5: Saturation porosity values (i/v) for all nine trial mixes

Trial	Saturation porosity
T1	0.34
T2	0.26
T3	0.19
T4	0.25
T5	0.21
T6	0.19
T7	0.27
T8	0.25
T9	0.23

Across the entire test program, saturation values ranged between 0.19 and 0.34. Trial 6 (W/C = 0.4) recorded the lowest saturation index of 0.19, pointing to a well-compacted internal structure that offered considerable resistance to water penetration — an outcome that closely aligns with Trial 6 also delivering the highest compressive strength of 29.5 N/mm². The PCE-based superplasticizer and silica fume combination clearly played a central role in densifying the pore network and reducing water ingress. What is particularly notable is that Trial 1 (W/C = 0.3), despite having the lowest w/c ratio, returned a higher saturation value of 0.34, largely owing to a substantial oven-dry weight loss of 140 g — suggesting a greater proportion of open, accessible pores in that mix. Mixes at W/C = 0.5 returned values between 0.23 and 0.27, confirming that excess water content leaves behind more pore space in the hardened concrete. The daily weight readings showed that absorption was most rapid during the first three days of immersion and stabilized by Day 5–Day 6, with all specimens effectively reaching moisture equilibrium well within the test period.

COMPARATIVE DISCUSSION

The results of the present study align well with prior research on 3D concrete printing mix optimization. Le et al. [1] reported optimal performance with a blend of 70% OPC, 20% fly ash, and 10% silica fume, a composition broadly consistent with the material proportions used in Trials 1–3 of this study. The optimum w/c ratio of 0.40 identified here also falls within the commonly recommended range of 0.35–0.45 for 3DCP mixes [3][15].

The Taguchi L9 experimental framework proved effective in identifying superplasticizer dosage as the single most influential factor affecting compressive strength, particularly at intermediate w/c ratios. This is consistent with the findings of Papachristoforou et al. [22], who demonstrated the efficiency of Taguchi-based designs in evaluating multiple interacting parameters simultaneously. Shaju et al. [25] reported 28-day compressive strengths of 27–35 MPa for mixes containing 25–35% fly ash, values that are comparable to the 29.5 N/mm² achieved in Trial 6 of this study.

The ImageJ porosity results support the observations of Putten et al. [16], who reported that lower w/c ratios and supplementary cementitious materials reduce macroporosity and strengthen interlayer bonding in printed elements. Similarly, the sorptivity outcomes echo the findings of Rahul et al. [13], underscoring that the combined effect of w/c ratio and mineral additives governs capillary network connectivity in extrudable concrete mixes.

CONCLUSION

This study systematically evaluated the effect of the w/c ratio and a combination of chemical and mineral additives on the mechanical and durability performance of 3D printable concrete, using a Taguchi L9 experimental design. The following key conclusions emerge from the results:

1. Trial 6 (w/c = 0.40, SP = 1.9%, SF = 0.2%, fiber = 0.65%, fly ash = 20%) delivered the best overall performance, achieving the highest 28-day compressive strength of 29.5 N/mm², the lowest saturation index of 0.19, and a moderate sorptivity coefficient - establishing it as the optimum mix for 3D concrete printing applications.
2. Trial 1 (w/c = 0.30) produced the densest surface pore structure with the lowest porosity of 32.02% and the smallest average pore size of 493 px² as determined by ImageJ analysis, indicating strong potential for long-term durability.
3. The sorptivity test confirmed that lower w/c ratios yield slower and lower total water uptake; however, the additive combination - particularly SP dosage - was found to be equally important in governing absorption behavior.
4. Silica fume at moderate dosages (0.2–5.1%) improved compressive strength and reduced permeability, while excessive dosages (10%) at low w/c ratios caused over-stiffening and unexpected strength reductions.
5. The saturation test confirmed that all nine mixes reached moisture equilibrium by Day 5–6 of continuous immersion, with negligible further weight gain thereafter — a reassuring indicator of long-term stability under wet service conditions.
6. The results consistently point to Trial 6 (W/C = 0.4) as the recommended mix design for 3D printable concrete, offering the most favorable combination of printability, mechanical strength, and durability across all four assessment methods used in this study.

REFERENCES

[1] T. T. Le, S. A. Austin, S. Lim, R. A. Buswell, R. Law, A. G. Gibb, and T. Thorpe, "Hardened properties of high-performance printing concrete," Cement and Concrete Research, vol. 42, no. 3, pp. 558–566, 2012.

[2] A. Kazemian, X. Yuan, E. Cochran, and B. Khoshnevis, "Cementitious materials for construction-scale 3D printing: Laboratory testing of fresh printing mixture," Construction and Building Materials, vol. 145, pp. 639–647, 2017.

[3] C. Zhang, Z. Hou, C. Chen, Y. Zhang, V. Mechtcherine, and Z. Sun, "Design of 3D printable concrete based on the relationship between flowability of cement paste and optimum aggregate content," Cement and Concrete Composites, vol. 104, p. 103406, 2019.

[4] K. Manikandan, K. Wi, X. Zhang, K. Wang, and H. Qin, "Characterizing cement mixtures for concrete 3D printing," Manufacturing Letters, vol. 24, pp. 33–37, 2020.

[5] G. Giridhar, P. R. Prem, and S. Kumar, "Development of concrete mixes for 3D printing using simple tools and techniques," Sadhana, vol. 48, no. 1, p. 16, 2023.

[6] M. K. Mohan, A. V. Rahul, G. De Schutter, and K. Van Tittelboom, "Early age hydration, rheology and pumping characteristics of CSA cement-based 3D printable concrete," Construction and Building Materials, vol. 275, p. 122136, 2021.

[7] Y. Zhang, Y. Zhang, G. Liu, Y. Yang, M. Wu, and B. Pang, "Fresh properties of a novel 3D printing concrete ink," Construction and Building Materials, vol. 174, pp. 263–271, 2018.

[8] I. Navarrete, Y. Kurama, N. Escalona, and M. Lopez, "Impact of physical and physicochemical properties of supplementary cementitious materials on structural build-up of cement-based pastes," Cement and Concrete Research, vol. 130, p. 105994, 2020.

[9] B. Panda, J. H. Lim, and M. J. Tan, "Mechanical properties and deformation behaviour of early age concrete in the context of digital construction," Composites Part B: Engineering, vol. 165, pp. 563–571, 2019.

[10] M. Papachristoforou, V. Mitsopoulos, and M. Stefanidou, "Evaluation of workability parameters in 3D printing concrete," Procedia Structural Integrity, vol. 10, pp. 155–162, 2018.

[11] J. V. D. Putten, M. Deprez, V. Cnudde, G. De Schutter, and K. Van Tittelboom, "Microstructural characterization of 3D printed cementitious materials," Materials, vol. 12, no. 18, p. 2993, 2019.

[12] ASTM C1585-20, "Standard Test Method for Measurement of Rate of Absorption of Water by Hydraulic-Cement Concretes," ASTM International, West Conshohocken, PA, 2020.

[13] A. V. Rahul, A. Sharma, and M. Santhanam, "A desorptivity-based approach for the assessment of phase separation during extrusion of cementitious materials," Cement and Concrete Composites, vol. 108, p. 103546, 2020.

[14] N. Roussel, "Rheological requirements for printable concretes," Cement and Concrete Research, vol. 112, pp. 76–85, 2018.

[15] G. Girskas and M. Kligys, "3D Concrete Printing Review: Equipment, Materials, Mix Design, and Properties," Buildings, vol. 15, p. 2049, 2025.

[16] J. Ye, C. Cui, J. Yu, K. Yu, and F. Dong, "Effect of polyethylene fiber content on workability and mechanical-anisotropic properties of 3D printed ultra-high ductile concrete," Construction and Building Materials, vol. 281, p. 122586, 2021.

[17] Y. Zhang, C. Zhang, G. Liu, Y. Yang, M. Wu, and B. Pang, "Fresh properties of a novel 3D printing concrete ink," Construction and Building Materials, vol. 174, pp. 263–271, 2018.

[18] IS 4031 (Part 6)-1988, "Methods of Physical Tests for Hydraulic Cement — Part 6: Determination of Compressive Strength of Hydraulic Cement," Bureau of Indian Standards, New Delhi, 1988.

[19] Y. Chen, S. C. Figueireo, C. Yalcinkaya, O. Copuroglu, F. Veer, and E. Schlangen, "The effect of viscosity-modifying admixture on the extrudability of limestone and calcined clay-based cementitious material for 3D concrete printing," Materials, vol. 12, no. 9, p. 1374, 2019.

[20] C. Wang, B. Chen, T. Vo, and M. Rezania, "Mechanical anisotropy, rheology and carbon footprint of 3D printable concrete: A review," Journal of Building Engineering, vol. 76, p. 107309, 2023.

[21] M. K. Mohan, A. V. Rahul, K. Van Tittelboom, and G. De Schutter, "Evaluating the influence of aggregate content on pumpability of 3D printable concrete," in Proc. 2nd RILEM Int. Conf. Concrete and Digital Fabrication, Springer, 2020, pp. 333–341.

[22] N. Khalil, G. Aouad, K. El Cheikh, and S. Remond, "Use of calcium sulfoaluminate cements for setting control of 3D-printing mortars," Construction and Building Materials, vol. 157, pp. 382–391, 2017.

[23] G. Bai, L. Wang, G. Ma, J. Sanjayan, and M. Bai, "3D printing eco-friendly concrete containing under-utilised and waste solids as aggregates," Cement and Concrete Composites, vol. 120, p. 104037, 2021.

[24] A. M. Neville, Properties of Concrete, 5th ed. Harlow, UK: Pearson Education Limited, 2011.

[25] G. Shaju, M. Raj, M. F. K. I, and A. K. A. A., "3D Printable Concrete Using Various Mix Designs," International Journal of Creative Research Thoughts (IJCRT), vol. 13, no. 3, pp. i836–i843, Mar. 2025.